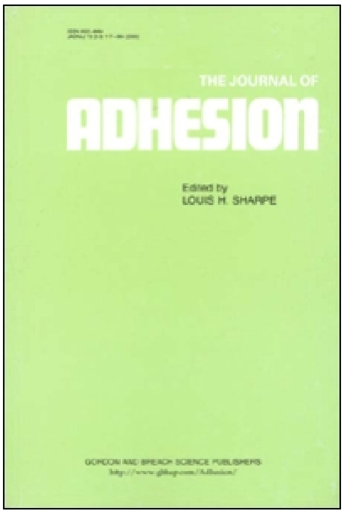

The Journal of Adhesion
Publication details, including instructions for authors and subscription information:
http://www.informaworld.com/smpp/title~content=t713453635

Vibration and Damping Characteristics of a Beam with a Partially Sandwiched Viscoelastic Layer

Tae-Hak Park[a]
[a] Agency for Defense Development, Yuseong, Taejon, Korea

To cite this Article Park, Tae-Hak(1997) 'Vibration and Damping Characteristics of a Beam with a Partially Sandwiched Viscoelastic Layer', The Journal of Adhesion, 61: 1, 97 — 122
To link to this Article: DOI: 10.1080/00218469708010518
URL: http://dx.doi.org/10.1080/00218469708010518

J. Adhesion, 1997, Vol. 61, pp. 97–122
Reprints available directly from the publisher
Photocopying permitted by license only

Vibration and Damping Characteristics of a Beam with a Partially Sandwiched Viscoelastic Layer

TAE-HAK PARK

Agency for Defense Development, P.O. Box 35, Yuseong, Taejon, 305-600, Korea

(Received 13 February 1996; In final form 28 May 1996)

The purpose of this study is to verify the vibration and damping characteristics of a partially-layered elastic-viscoelastic-elastic structure both theoretically and experimentally.

The fourth-order differential equations of motion are derived for the transverse vibration of a three-layered sandwich beam with a viscoelastic (or adhesive) core layer. The transverse displacements of the constraining layer and the base beam are assumed to have different parameters. Both the transverse normal strain and the longitudinal shear strain of the viscoelastic core layer are included in the equations of motion. The solution to the resulting equations is obtained by solving a boundary value problem.

Numerical analysis of the equations and experimental measurements is illustrated by a cantilever beam in transverse vibration.

The vibration and damping effects of completely and partially covered beams are investigated and the effect of the position changes of partial coverage is intensively analyzed.

Keywords: Vibration; damping; viscoelastic layer; constraining layer; partial coverage; three-layered beam; completely covered beam

1. INTRODUCTION

It has long been observed that structural vibration and noise can be reduced by utilizing adhesive layers to dissipate energy within vibrating members [1–13]. Such reductions are of practical interest in design applications where resonant excitation cannot be avoided.

Especially, amplitude reduction at the resonant frequency and the movement of the natural frequency are very important design factors which should be considered when structures are subject to dynamic environments. A large number of papers on sandwich structures have been reported as follows.

Ditaranto [1] studied damped sandwich beams with arbitrary boundary conditions. He derived the sixth-order differential equation of motion in terms of longitudinal displacement for a freely vibrating beam which considered shear deformation effects. Mead and Markus [2] derived the sixth-order differential equation in terms of the transverse motion for a three-layered beam in forced vibration which considered shear deformation effects. Yan and Dowell [3] suggested an analytical method which considered the longitudinal displacements and the rotary inertias of all the layers of a three-layered beam and the shear strain of the base beam and the constraining layer. Douglas and Yang [4] derived the eighth-order differential equation for a three-layered beam which considered the normal deformation effects of a viscoelastic (or adhesive) layer in forced vibration. Okazaki and Urata [5, 6] studied the damping characteristics of two-layered curved beams and cylindrically curved plates with an unconstrained viscoelastic layer. Rao and Crocker [7] analyzed the effects of viscoelastic material on the natural frequencies of a simply-supported beam with a lap joint.

Plunkett and Lee [8] studied the damping effects of a three-layered beam with a fully covered viscoelastic layer and a partially covered constraining layer. Okazaki and Urata [9] derived the second order differential equation which considered the longitudinal deformations of a base beam and a constraining layer, and the fourth-order differential equation which considered the transverse deformation of both ends of a fixed beam which was partially covered at the center. Dewa, Okada and Nagai [10] studied the damping effects in cases of both ends of the viscoelastic layer being free and both ends being constrained.

In this paper, the vibration and damping characteristics of a partially-covered elastic-viscoelastic-elastic beam were investigated theoretically and experimentally. The fourth order differential equations of motion are derived from the transverse vibration of a three-layered sandwich beam with a viscoelastic (or adhesive) core layer.

Most of the previous studies of the partially-covered beam [8–10] were mainly interested in the maximum damping effects due to the shear deformation of the viscoelastic layer with the change of the constraining layer's length and boundary condition. But, in this paper, both the transverse normal deformation and the longitudinal shear deformation of a viscoelastic core layer are considered. The transverse displacements of the constraining layer and the base beam are assumed to have different parameters. The solution of the equations of motion is obtained by solution of a boundary value problem. The vibration and damping effects of completely- and partially-covered beams are investigated and the effect of the position changes of a partial coverage is intensively analyzed.

2. THEORY

The equations of motion of the three-layered beam, as shown in Figure 1, are derived based on the following assumptions.

1) The viscoelastic (or adhesive) layer is modeled as a distributed linearly viscoelastic spring which transmits shear and normal stresses between adjacent elastic layers.
2) The continuity of displacements and stresses at contact points between viscoelastic layer and elastic layers are preserved.
3) The transverse displacements of elastic layers are different from each other.
4) The base beam and the constraining layer are treated as Bernoulli-Euler beams.
5) The mass of the viscoelastic layer is neglected because it is very small and light compared with the base beam.

2.1. Relation of the Displacement and Strain of the Viscoelastic Layer

The x-directional displacements at the top and the bottom of elastic layer 1 and 2 in Figure 1(b), u_{1t} and u_{2b} are given as

$$u_{1t} = -\frac{h_1}{2}\theta_1 \tag{1}$$

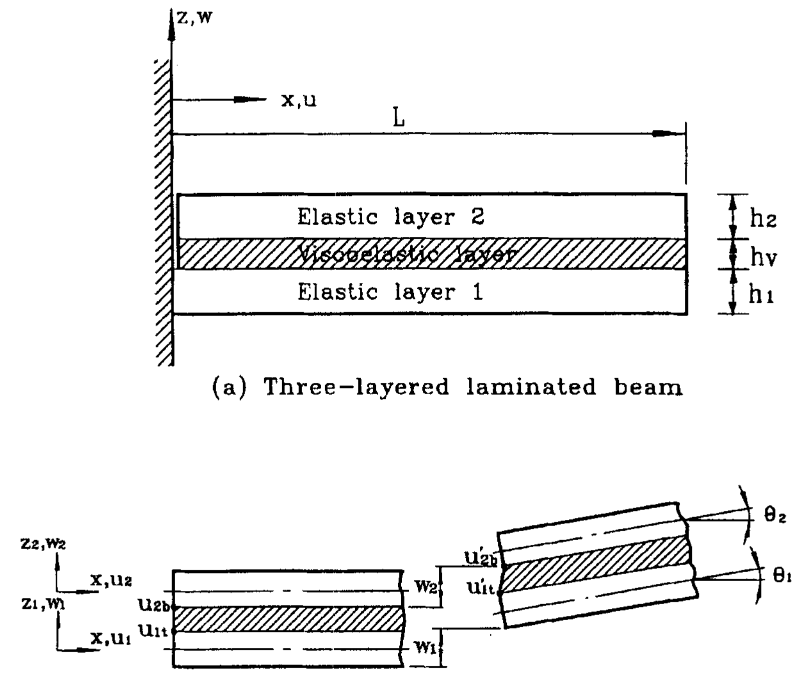

FIGURE 1 Geometry and coordinate system for a three-layered beam, undeformed and deformed.

$$u_{2b}=\frac{h_2}{2}\theta_2 \tag{2}$$

where $\theta_i (i=1,2)$ is a rotation angle of the neutral axis of the elastic layer i. In the x-directional displacement, the bottom of the viscoelastic layer is equal to the top of elastic layer 1 and the top of the viscoelastic layer is equal to the bottom of elastic layer 2.

The relation of displacement and strain is given as

$$\gamma_v(x)=\frac{u_{2b}-u_{1t}}{h_v}=\frac{h_2\theta_2+h_1\theta_1}{2\,h_v} \tag{3}$$

$$\varepsilon_v(x)=\varepsilon_z(x)=\frac{w_2-w_1}{h_v} \tag{4}$$

where h_v, $\gamma_v(x)$ and $\varepsilon_v(x)$ are the thickness, shear strain and normal strain of the viscoelastic layer and, $w_i\,(i=1,2)$ is the z-directional displacement of elastic layer i.

2.2. Relation of the Stress and Strain of the Viscoelastic Layer

The relation of the stress and strain of the viscoelastic layer is given as

$$\tau_v(x) = G_v\, \gamma_v(x) \tag{5}$$

$$\sigma_v(x) = E_v\, \varepsilon_v(x) \tag{6}$$

where $\tau_v(x)$, $\sigma_v(x)$, E_v and G_v are shear stress, normal stress, Young's modulus and shear modulus of the viscoelastic layer. We assume that the viscoelastic material is isotropic and incompressible. Then Poisson's ratio μ is 0.5 and the relation of Young's and shear modulus becomes $E_v = 3G_v$.

Substituting Eq. (3) and Eq. (4) into Eq. (5) and Eq. (6), the results are expressed as

$$\tau_v = \frac{G_v(h_1\,\theta_1 + h_2\,\theta_2)}{2\,h_v} \tag{7}$$

$$\sigma_v = \frac{E_v(w_2 - w_1)}{h_v} \tag{8}$$

2.3. Equilibrium Equations

1) Equilibrium equations of beam 1

From beam 1 in Figure 2, the sum of the z-directional forces is written as

$$\sum F_z = \frac{\partial Q_{x1}}{\partial x}dx + \sigma_v(x)\,dx - F^I_{z1}\,dx = 0 \tag{9}$$

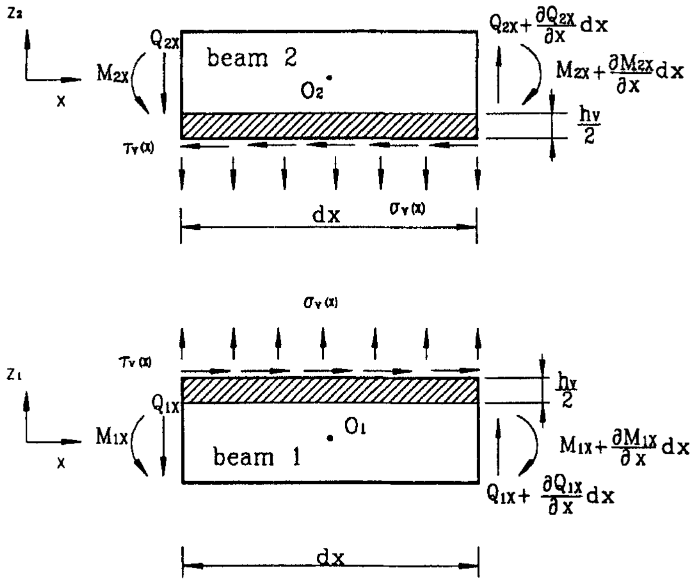

FIGURE 2 Force equilibrium for a differential volume of beam.

where F^I_{z1} is the z-directional inertia force of beam 1 per unit width in the y-direction and unit length in the x-direction.

$$F^I_{z1} = \rho h_1 \ddot{w}_1 = \rho_1 h_1 \frac{\partial^2 w_1(x,t)}{\partial t^2} \tag{10}$$

Substituting eq. (8) and eq. (10) into eq. (9) and rearranging it, we obtain eq. (11):

$$\begin{aligned}\frac{\partial Q_{x1}}{\partial x} &= -\frac{E_v}{h_v}(w_2 - w_1) + \rho_1 h_1 \ddot{w}_1 \\ &= \left(\frac{E_v}{h_v} w_1 + \rho_1 h_1 \ddot{w}_1\right) - \frac{E_v}{h_v} w_2\end{aligned} \tag{11}$$

Assuming that clockwise rotation is positive, moment equilibrium is expressed as

$$\sum M_{01} = \frac{\partial M_{x1}}{\partial x} dx - Q_{x1} dx + \tau_v(x) dx \left(\frac{h_1}{2} + \frac{h_v}{2}\right) = 0 \tag{12}$$

Substituting Eq. (7) into Eq. (12) and rearranging it, the results are written as

$$\frac{\partial M_{x1}}{\partial x} - Q_{x1} + \frac{G_v(h_1 + h_v)h_1}{4h_v}\theta_1 + \frac{G_v(h_1 + h_v)h_2}{4h_v}\theta_2 = 0 \quad (13)$$

2) Equilibrium equations of beam 2

From beam 2 in Figure 2, the sum of the z-directional forces is shown as

$$\sum F_z = \frac{\partial Q_{x2}}{\partial x}dx - \sigma_v(x)\,dx - F^I_{z2}\,dx = 0 \quad (14)$$

Substituting Eq. (8) into Eq. (14) and rearranging it, it can be written as

$$\frac{\partial Q_{x2}}{\partial x} = \frac{E_v}{h_v}(w_2 - w_1) + \rho_2 h_2 \ddot{w}_2$$

$$= \left(\frac{E_v w_2}{h_v} + \rho_2 h_2 \ddot{w}_2\right) - \frac{E_v w_1}{h_v} \quad (15)$$

The moment equilibrium of mass center o_2 is given as

$$\sum M_{02} = \frac{\partial M_{x2}}{\partial x}dx - Q_{x2}dx + \tau_v(x)\,dx\left(\frac{h_2}{2} + \frac{h_v}{2}\right) = 0 \quad (16)$$

Substituting Eq. (7) into Eq. (16) and rearranging it, the results are shown as

$$\frac{\partial M_{x2}}{\partial x} - Q_{x2} + \frac{G_v(h_2 + h_v)h_1}{4h_v}\theta_1 + \frac{G_v(h_2 + h_v)h_2}{4h_v}\theta_2 = 0 \quad (17)$$

2.4. Equations of Motion

Differentiating Eq. (13) with respect to x in order to derive an equation of motion of the system, the results are

$$\frac{\partial^2 M_{x1}}{\partial x^2} - \frac{\partial Q_{x1}}{\partial x} + \frac{G_v(h_1 + h_v)h_1}{4h_v}\frac{\partial \theta_1}{\partial x} + \frac{G_v(h_1 + h_v)h_2}{4h_v}\frac{\partial \theta_2}{\partial x} = 0 \quad (18)$$

where

$$\theta_i = \frac{\partial w_i}{\partial x} \tag{19}$$

$$M_{xi} = -E_i I_i \frac{\partial^2 w_i}{\partial x^2}, \quad i = 1,2 \tag{20}$$

Substituting Eq. (11), Eq. (19) and Eq. (20) into Eq. (18) and rearranging it, the results are shown as

$$E_1 I_1 \frac{\partial^4 w_1}{\partial x^4} - R_1 h_1 \frac{\partial^2 w_1}{\partial x^2} - R_1 h_2 \frac{\partial^2 w_2}{\partial x^2} + \frac{E_v}{h_v} w_1 - \frac{E_v}{h_v} w_2 + \rho_1 h_1 \ddot{w}_1 = 0 \tag{21}$$

where

$$R_i = \frac{G_v(h_i + h_v)}{4 h_v}, \quad i = 1,2 \tag{22}$$

Treating beam 2 in a similar manner, the results are

$$E_2 I_2 \frac{\partial^4 w_2}{\partial x^4} - R_2 h_1 \frac{\partial^2 w_1}{\partial x^2} - R_2 h_2 \frac{\partial^2 w_2}{\partial x^2} - \frac{E_v}{h_v} w_1 + \frac{E_v}{h_v} w_2 + \rho_2 h_2 \ddot{w}_2 = 0 \tag{23}$$

The solutions of Eq. (21) and Eq. (23) are assumed to be harmonic functions as follows:

$$w_1 = W_1(x) e^{iwt} \tag{24}$$

$$w_2 = W_2(x) e^{iwt} \tag{25}$$

Substituting Eq. (24) and Eq. (25) into Eq. (21) and Eq. (23), the equations of motion are given as

$$E_1 I_1 \frac{\partial^4 W_1}{\partial x^4} - R_1 h_1 \frac{\partial^2 W_1}{\partial x^2} - R_1 h_2 \frac{\partial^2 W_2}{\partial x^2} + \left(\frac{E_v}{h_v} - \rho_1 h_1 \omega^2\right) W_1 - \frac{E_v}{h_v} W_2 = 0 \tag{26}$$

$$E_2I_2\frac{\partial^4 W_2}{\partial x^4}-R_2h_1\frac{\partial^2 W_1}{\partial x^2}-R_2h_2\frac{\partial^2 W_2}{\partial x^2}+\left(\frac{E_v}{h_v}-\rho_2h_2\omega^2\right)W_2 -\frac{E_v}{h_v}W_1=0 \tag{27}$$

The solutions of Eq. (26) and (27) are assumed to be harmonic functions as follows:

$$W_1(x)=A\,e^{\lambda x} \tag{28}$$

$$W_2(x)=B\,e^{\lambda x} \tag{29}$$

where constants A and B should be determined by boundary conditions.

Substituting Eq. (28) and Eq. (29) into Eq. (26) and Eq. (27), we obtain a matrix of the form:

$$\begin{bmatrix} E_1I_1\lambda^4-R_1h_1\lambda^2+\left(\frac{E_v}{h_v}-\rho_1h_1\omega^2\right) & -R_1h_2\lambda^2-\frac{E_v}{h_v} \\ -R_2h_1\lambda^2-\frac{E_v}{h_v} & E_2I_2\lambda^4-R_2h_2\lambda^2+\left(\frac{E_v}{h_v}-\rho_2h_2\omega^2\right)\end{bmatrix}\begin{bmatrix}A\\B\end{bmatrix}=0 \tag{30}$$

For a nontrivial solution, the determinant of the above matrix is set equal to zero yielding eight roots of λ. Finally, we have

$$W_1(x)=\sum_{n=1}^{8}A_n\,e^{\lambda_n x} \tag{31}$$

$$W_2(x)=\sum_{n=1}^{8}B_n\,e^{\lambda_n x}=\sum_{n=1}^{8}\Phi_n\,A_n\,e^{\lambda_n x} \tag{32}$$

where

$$\Phi_n=\frac{R_2h_1\lambda_n^2+\frac{E_v}{h_v}}{E_2I_2\lambda_n^4-R_2h_2\lambda_n^2+\left(\frac{E_v}{h_v}-\rho_2h_2\omega^2\right)} \tag{33}$$

3. APPLICATION OF THE EQUATIONS OF MOTION

3.1. Completely Covered Cantilever Beam

If the harmonic excitation $F = F_o e^{iwt}$ is applied at the free edge of the cantilever beam as in Figure 3(a), the steady state solution of the beam can be solved as a boundary value problem.

The boundary conditions are as follows:

1) at $x = 0$

$$w_1 = \sum_{n=1}^{8} A_n = 0 \tag{34}$$

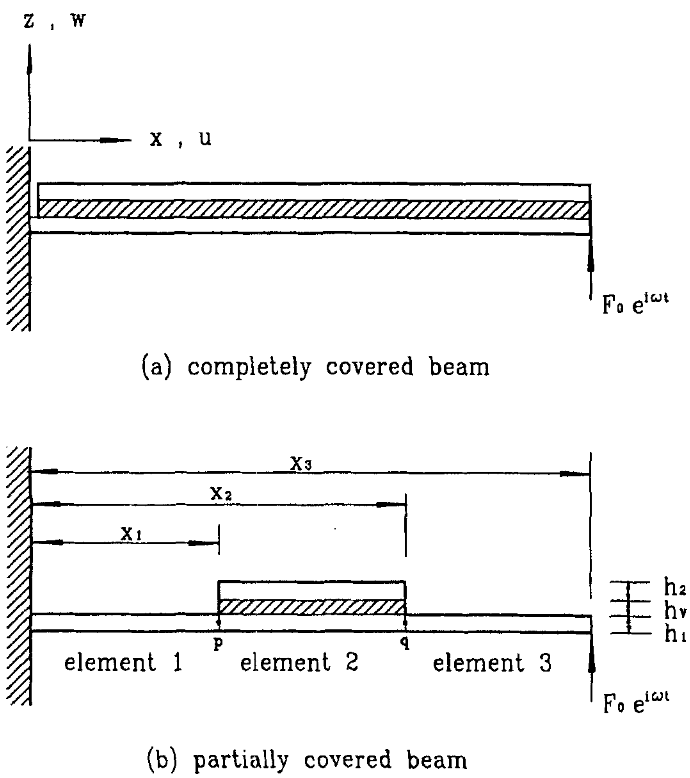

FIGURE 3 Geometry and coordinate system of beam specimen.

$$\frac{\partial w_1}{\partial x} = \sum_{n=1}^{8} \lambda_n A_n = 0 \tag{35}$$

$$\frac{\partial^2 w_2}{\partial x^2} = \sum_{n=1}^{8} \Phi_n \lambda_n^2 A_n = 0 \tag{36}$$

$$\frac{\partial^3 w_3}{\partial x^3} = \sum_{n=1}^{8} \Phi_n \lambda_n^3 A_n = 0 \tag{37}$$

2) at $x = 1$

$$\frac{\partial^2 w_1}{\partial x^2} = \sum_{n=1}^{8} \lambda_n^2 e^{\lambda_n 1} A_n = 0 \tag{38}$$

$$\frac{\partial^3 w_1}{\partial x^3} = \frac{F}{E_1 I_1} \tag{39}$$

$$\frac{\partial^2 w_2}{\partial x^2} = \sum_{n=1}^{8} \Phi_n \lambda_n^2 e^{\lambda_n 1} A_n = 0 \tag{40}$$

$$\frac{\partial^3 w_2}{\partial x^3} = \frac{m}{E_2 I_2} \frac{\partial^2 w_2}{\partial t^2} \tag{41}$$

The mass of an accelerometer attached at the free edge of the cantilever beam, m is included in the right term of Eq. (41).

Getting A_n from Eq. (34) through (41) and substituting the results into Eq. (24) and Eq. (25), the steady state solution is obtained.

$$w_1 = W_1 e^{i\omega t} = \left(\sum_{n=1}^{8} A_n e^{\lambda_n x} \right) e^{i\omega t} \tag{42}$$

$$w_2 = W_2 e^{i\omega t} = \left(\sum_{n=1}^{8} \Phi_n A_n e^{\lambda_n x} \right) e^{i\omega t} \tag{43}$$

3.2. Partially-covered Cantilever Beam

If the external force $F = F_o e^{i\omega t}$ is applied at the free edge of a partially-covered cantilever beam as in Figure 3(b), the solution of element 2 is the same as Eq. (42) and Eq. (43). The equations of motion of element 1 and element 3 are given as

$$E_{bj} I_{bj} \frac{\partial^4 w_{bj}}{\partial x_j^4} + \rho_{bj} h_{bj} \frac{\partial^2 w_{bj}}{\partial t^2} = 0, \quad j = 1,3 \tag{44}$$

The solution of Eq. (44) is assumed as follows:

$$w_{bj} = W_{bj}(x)\, e^{i\omega t} = W_{bj} e^{i\omega t} \tag{45}$$

where w_{bj} is the z-directional displacement of element j. Substituting Eq. (45) into Eq. (44), we obtain

$$\frac{\partial^4 W_{bj}}{\partial x_j^4} - \frac{\rho_{bj} h_{bj}}{E_{bj} I_{bj}} \omega^2 W_{bj} = 0 \tag{46}$$

The solutions of Eq. (46) are assumed as follows:

$$W_{b1} = \sum_{n=1}^{4} C_n e^{\beta_n x}, \quad 0 < x < x_1 \tag{47}$$

$$W_{b3} = \sum_{n=1}^{4} D_n e^{\beta_n x}, \quad x_2 < x < x_3 \tag{48}$$

As elements 1, 2 and 3 should satisfy continuity conditions at points p and q of the base beam in Figure 3(b), displacements of the elements should be the same at those points. The same can be applied to slopes, moments and shear forces.

1) at $x = x_1$

$$w_{b1} = w_1 ; \sum_{n=1}^{4} C_n e^{\beta_n x_1} = \sum_{n=1}^{8} A_n e^{\lambda_n x_1} \tag{49}$$

$$\frac{\partial w_{b1}}{\partial x}=\frac{\partial w_1}{\partial x};\ \sum_{n=1}^{4}\beta_n C_n e^{\beta_n x_1}=\sum_{n=1}^{8}\lambda_n A_n e^{\lambda_n x_1} \tag{50}$$

$$\frac{\partial^2 w_{b1}}{\partial x^2}=\frac{\partial^2 w_1}{\partial x^2};\ \sum_{n=1}^{4}\beta_n^2 C_n e^{\beta_n x_1}=\sum_{n=1}^{8}\lambda_n^2 A_n e^{\lambda_n x_1} \tag{51}$$

$$\frac{\partial^3 w_{b1}}{\partial x^3}=\frac{\partial^3 w_1}{\partial x^3};\ \sum_{n=1}^{4}\beta_n^3 C_n e^{\beta_n x_1}=\sum_{n=1}^{8}\lambda_n^3 A_n e^{\lambda_n x_1} \tag{52}$$

2) at $x=x_2$

$$w_{b3}=w_1;\ \sum_{n=1}^{4}D_n e^{\beta_n x_2}=\sum_{n=1}^{8}A_n e^{\lambda_n x_2} \tag{53}$$

$$\frac{\partial w_{b3}}{\partial x}=\frac{\partial w_1}{\partial x};\ \sum_{n=1}^{4}\beta_n D_n e^{\beta_n x_2}=\sum_{n=1}^{8}\lambda_n A_n e^{\lambda_n x_2} \tag{54}$$

$$\frac{\partial^2 w_{b3}}{\partial x^2}=\frac{\partial^2 w_1}{\partial x^2};\ \sum_{n=1}^{4}\beta_n^2 D_n e^{\beta_n x_2}=\sum_{n=1}^{8}\lambda_n^2 A_n e^{\lambda_n x_2} \tag{55}$$

$$\frac{\partial^3 w_{b3}}{\partial x^3}=\frac{\partial^3 w_1}{\partial x^3};\ \sum_{n=1}^{4}\beta_n^3 D_n e^{\beta_n x_2}=\sum_{n=1}^{8}\lambda_n^3 A_n e^{\lambda_n x_2} \tag{56}$$

The boundary conditions are as follows:
3) at $x=0$

$$w_{b1}=\sum_{n=1}^{4}C_n=0 \tag{57}$$

$$\frac{\partial w_{b1}}{\partial x}=\sum_{n=1}^{4}\beta_n C_n=0 \tag{58}$$

4) at $x=x_1$

$$\frac{\partial^2 w_2}{\partial x^2}=\sum_{n=1}^{8}\lambda_n^2 \Phi_n A_n e^{\lambda_n x_1}=0 \tag{59}$$

$$\frac{\partial^3 w_2}{\partial x^3} = \sum_{n=1}^{8} \lambda_n^3 \Phi_n A_n e^{\lambda_n x_1} = 0 \tag{60}$$

5) at $x = x_2$

$$\frac{\partial^2 w_2}{\partial x^2} = \sum_{n=1}^{8} \lambda_n^2 \Phi_n A_n e^{\lambda_n x_2} = 0 \tag{61}$$

$$\frac{\partial^3 w_2}{\partial x^3} = \sum_{n=1}^{8} \lambda_n^3 \Phi_n A_n e^{\lambda_n x_2} = 0 \tag{62}$$

6) at $x = x_3$

$$\frac{\partial^2 w_{b_3}}{\partial x^2} = \sum_{n=1}^{4} \beta_n^2 D_n e^{\beta_n x_3} = 0 \tag{63}$$

$$\frac{\partial^2 w_{b_3}}{\partial x^3} = \frac{F}{E_{b3} I_{b3}} + \frac{m}{E_{b3} I_{b3}} \frac{\partial^2 w_{b3}}{\partial t^2} \tag{64}$$

The effect of the mass(m) of accelerometer is considered in the second term of the right side of Eq. (64). From Eq. (49) through (64), the undetermined constants C_n, D_n and A_n are obtained. Substituting them into Eq. (42), Eq. (43) and Eq. (45), displacement at arbitrary points can be calculated.

4. NUMERICAL ANALYSIS, EXPERIMENTS AND CONSIDERATIONS

Once the λ_n are known from Eq. (30), the constants A_n are obtained by boundary conditions. Then λ_n and A_n are substituted into Eq. (42) and Eq. (43), where the displacement are calculated.

Now, I am going to define an inertance that is one of frequency response functions to compare the damping characteristics of specimens. Inertance at an arbitrary point of the system is given as

$$\mathrm{INT}(x,\omega) = \frac{\ddot{w}_2(x)}{F_o e^{i\omega t}} = -\frac{\omega^2}{F_o}\left(\sum_{n=1}^{8} \Phi_n A_n e^{\lambda_n x}\right) = -\frac{\omega^2}{F_o} W_2(x) \tag{65}$$

A computer program has been developed in FORTRAN on a Cyber 180/860 system to perform the numerical solution. The configuration and physical properties of the completely-covered specimen are given in Table I. The thickness and properties of the elastic layers and the viscoelastic layer of partially-covered specimens are the same as those of the completely-covered specimen cs1. The position and length of the constraining layer is different as shown in Figure 4 and Figure 14.

The viscoelastic material chosen for study is production No. SJ2015X Type 112 of 3M Co. The dynamic shear modulus G_v, and loss factor, α, of the viscoelastic material are shown in Table I.

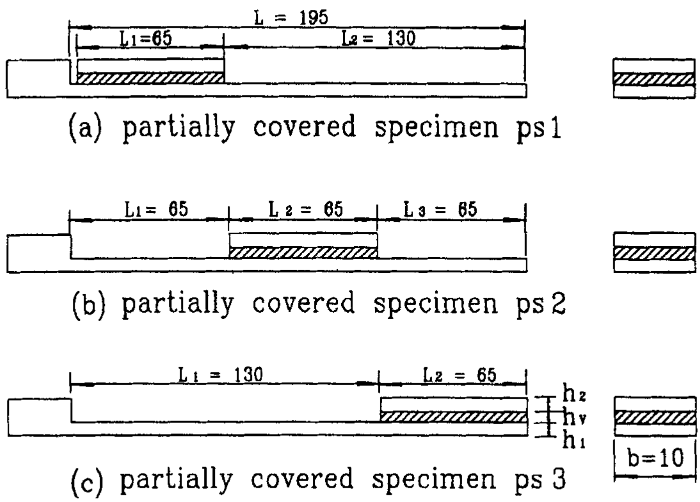

FIGURE 4 Partially-covered specimens (unit: mm).

TABLE I Dimensions and physical data of completely-covered beam specimen

Specimen and Physical data		*Dimensions (unit : mm)*				
		L	b	h_1	h_v	h_2
Specimen	cs1	195.00	10.00	2.00	1.00	2.00
Elastic beam		Steel AISI 4130 : $E = 1.99815 \times 10^{12}$ (dyne/cm^2)				
Viscoelastic material ($T = 23.88$°c)		Shear modulus: $G_v = (\text{freq.})^{0.557} \times 5.966 \times 10^5 \times (1. + i\alpha)$ (dyne/cm^2) Loss factor: $\alpha = 0.0520947 \times \ln(\text{freq.}) + 0.644273$				

Experiments were performed by impulse excitation [14] as in Figure 5. An impact hammer with an attached force transducer was used to excite specimens and the responses were measured using an accelerometer with a mass of 1 gram. The excitation and measuring points were the tip of the cantilever beam. The frequency responses between 0 and 5000 Hz were recorded by an FFT analyzer.

Figure 6 shows the theoretical and experimental results of a completely-covered specimen cs1. Agreement is seen to be good. These data will be used as a reference for the damping characteristics of partially-covered specimens.

Figures 7 through 9 show the theoretical and experimental results of partially-covered specimens ps1, ps2 and ps3, respectively. There is significant agreement between them in the measured frequency range. Most of the previous studies of the partially-covered beam [8–10] were mainly interested in the maximum damping effects due to the shear deformation of a viscoelastic layer with the change of the constraining layer's length and boundary condition. In this study, however, the

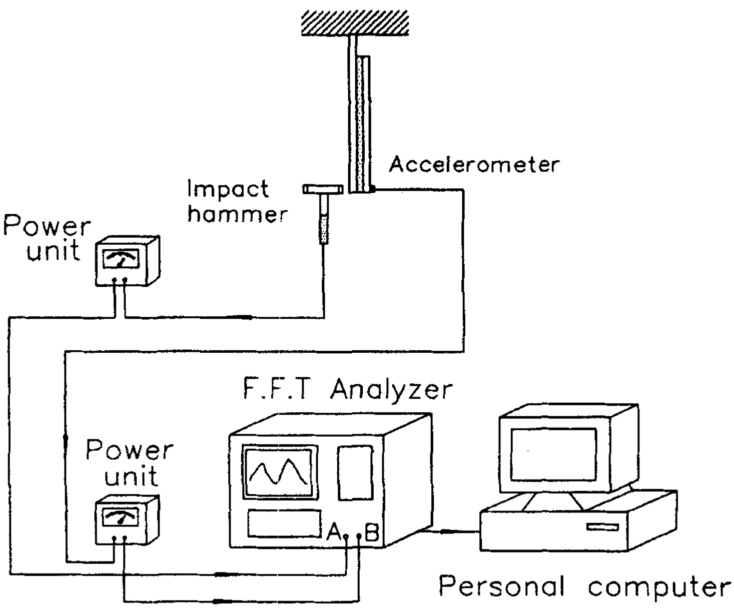

FIGURE 5 Experimental set-up.

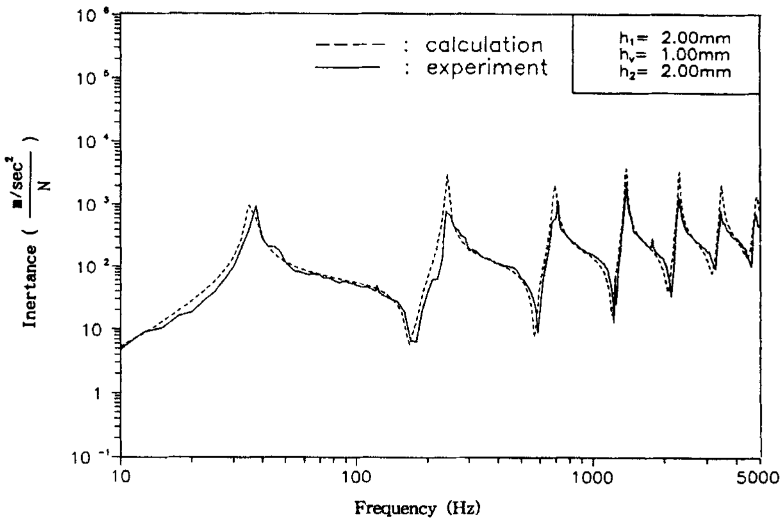

FIGURE 6 Transverse driving point inertance of completely-covered specimen cs1.

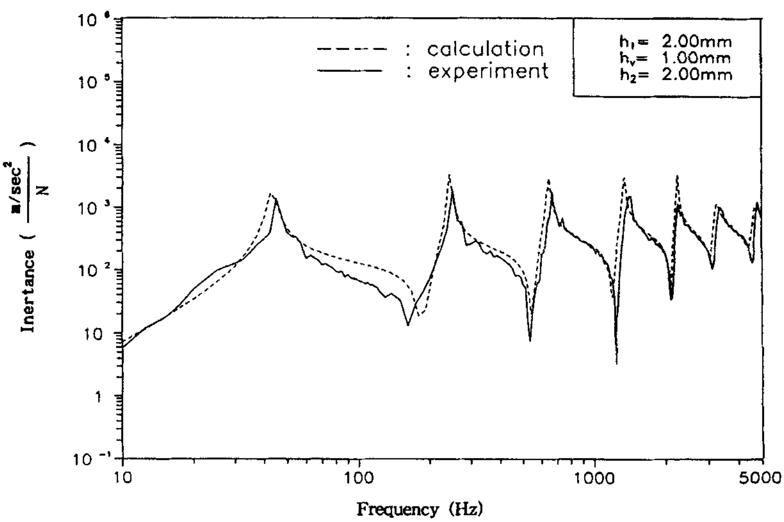

FIGURE 7 Transverse driving point inertance of partially-covered specimen ps1.

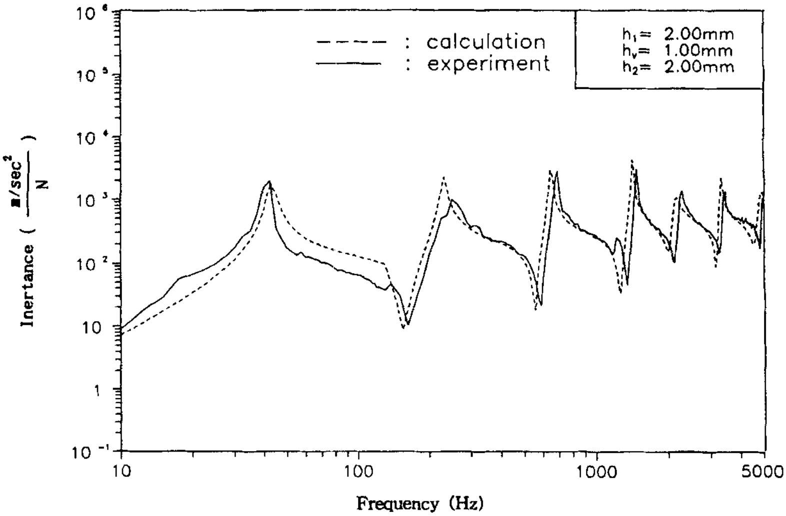

FIGURE 8 Transverse driving point inertance of partially-covered specimen ps2.

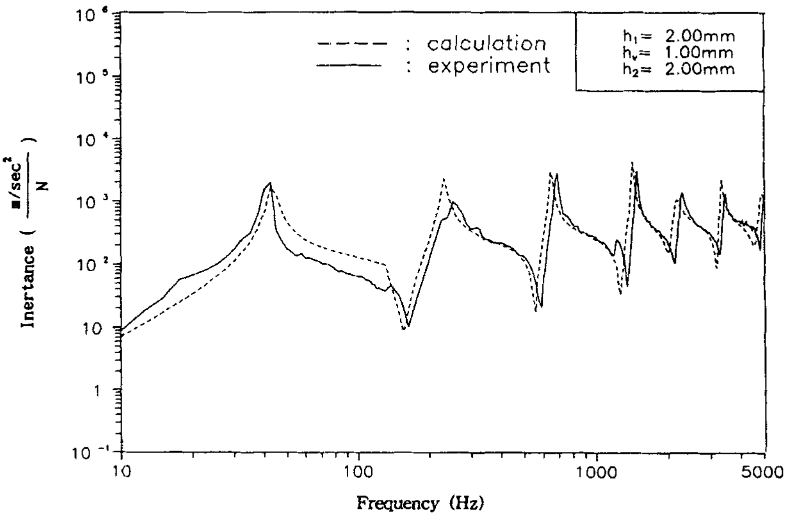

FIGURE 9 Transverse driving point inertance of partially-covered specimen ps3.

normal deformaion, as well as the shear deformation, was considered and the solution of the equations of motion was obtained by solving a boundary value problem. It was assumed that the transverse displacements of a base beam and a constraining layer had different parameters because of differing boundary conditions of the constraining layer and the base beam.

Figure 10 indicates the comparison of the transverse driving point inertances of a bare base beam and a completely-covered specimen cs1. The reduction of the system response at the resonant frequencies approaches 21 db on average. It shows that the damping effects of viscoelastic material are significant.

Normally, the design purpose of compositely layered structures is to minimize the weight and to maximize the damping effect of the system. Therefore, it is worth comparing and investigating the vibration and damping effects, and the weight reduction effects, between the partially-covered beams and the completely-covered beams.

Figures 11 through 13 show a comparison of the transverse driving point inertances of a completely-covered specimen cs1 and partially-covered specimens ps1, ps2 and ps3, respectively. The weight of each constraining layer of the partially-covered specimens is one-third that of the completely-covered specimen. The reduction of the system response at the resonant frequencies of each specimen approaches 20 db

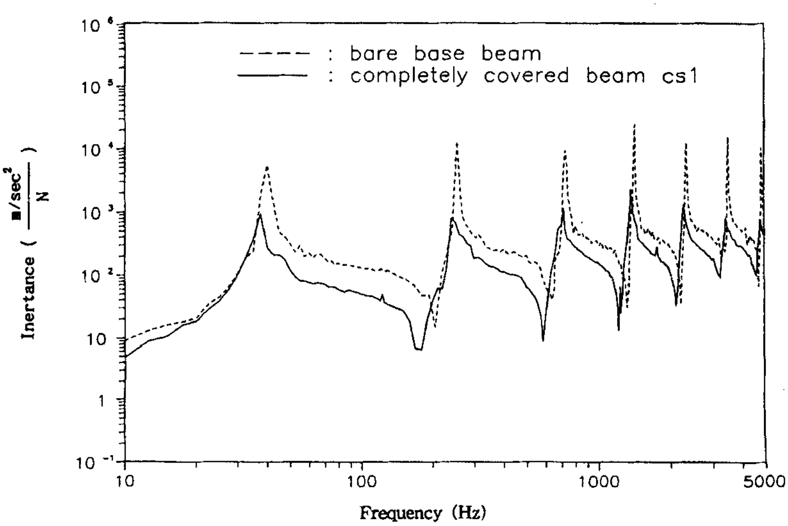

FIGURE 10 Comparison of transverse driving point inertances of bare-base beam and completely-covered specimen cs1.

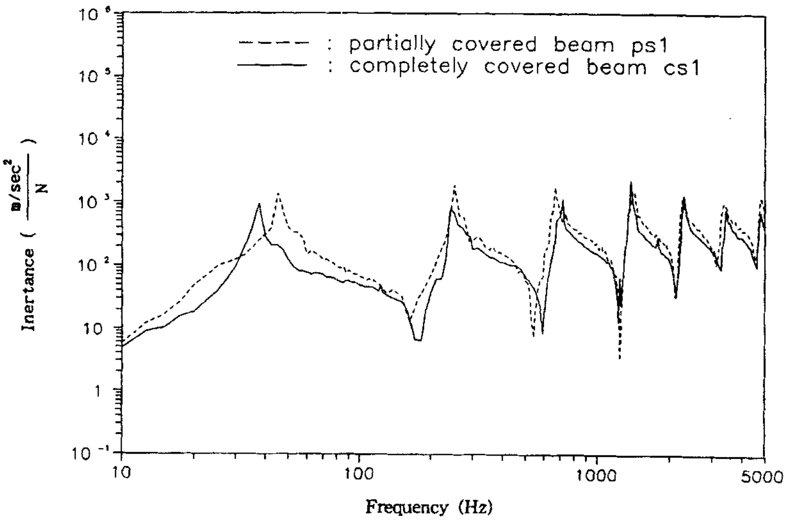

FIGURE 11 Comparison of transverse driving point inertances of completely- and partially-covered specimens cs1 and ps1.

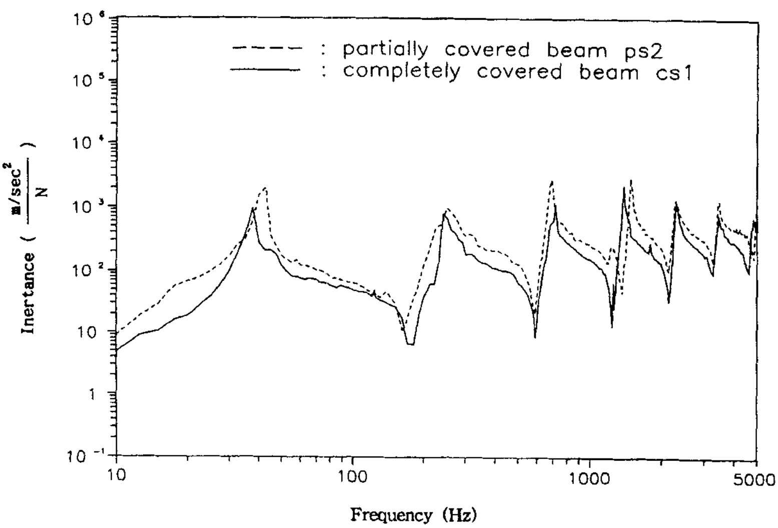

FIGURE 12 Comparison of transverse driving point inertances of completely- and partially-covered specimens cs1 and ps2.

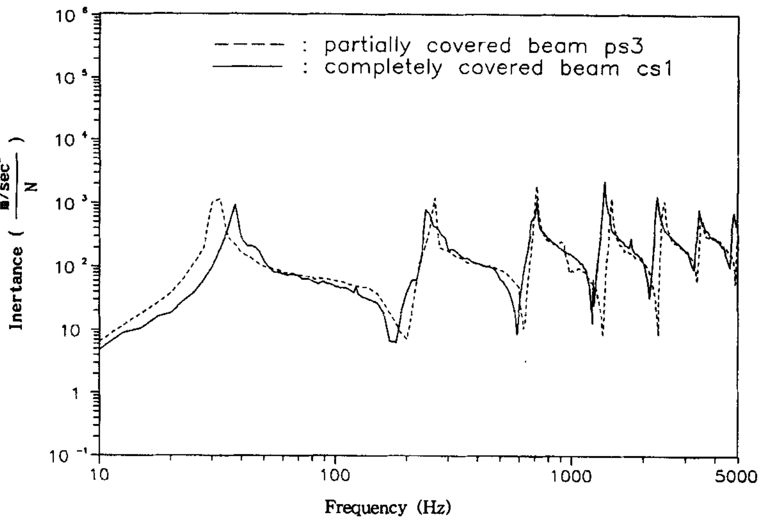

FIGURE 13 Comparison of transverse driving point inertances of completely- and partially-covered specimens cs1 and ps3.

on average, as shown in Table II. It is important to note that the damping effect of partially-covered specimens is very similar to that of a completely-covered specimen. In Table II, the damping effect of the partially-covered specimen ps3 is greater than that of ps1 and ps2 in the 1st resonant frequency and resonant frequencies greater than the 4th. Also, the movement of the 1st resonant frequency is larger when compared with the other specimens. This is a result of the concentrated mass effects of the free edge. In the case of a cantilever beam, it means that the vibration and damping effects are increased if the free edge is partially layered. The damping effect of ps2 is greater than ps1 or ps3 at the 2nd resonant frequency. This is because the partially-covered position is located at the center of the cantilever beam affecting the second mode shape.

From the above results, if the partial coverage is positioned near the free edge of the cantilever beam, the vibration and damping effects of the partially-covered beam are more significant and economical than those of the completely-covered beam. Consequently, it can be supposed that the vibration and damping control of a specific mode of a

TABLE II Resonant frequencies and inertances of cantilever beam specimens $\left(\text{Freq.: Hz, Inet.: } \frac{\text{m/sec}^2}{\text{N}}\right)$

No. of resonant frequency		*Type of specimen*						
		ps1	*ps2*	*ps3*	*ps4*	*ps5*	*cs1*	*bare base beam*
1st	Freq.	45.0	43.0	33.0	35.0	34.0	38.0	40.0
	Inet.	(1360.0)	(1990.0)	(1160.0)	(3620.0)	(3620.0)	(952.0)	(5440.0)
2nd	Freq.	250.0	250.0	263.0	213.0	213.0	240.0	255.0
	Inet.	(1870.0)	(992.0)	(1230.0)	(880.0)	(596.0)	(797.0)	(12900.0)
3rd	Freq.	663.0	688.0	713.0	675.0	600.0	713.0	725.0
	Inet.	(1790.0)	(2800.0)	(1930.0)	(1860.0)	(944.0)	(1150.0)	(9470.0)
4th	Freq.	1425.0	1475.0	1475.0	1350.0	1300.0	1375.0	1425.0
	Inet.	(1540.0)	(3020.0)	(1240.0)	(634.0)	(1180.0)	(2270.0)	(24600.0)
5th	Freq.	2250.0	2275.0	2450.0	2200.0	2200.0	2288.0	2350.0
	Inet.	(1150.0)	(1380.0)	(1110.0)	(422.0)	(622.0)	(1320.0)	(12900.0)
6th	Freq.	3350.0	3438.0	3500.0	3525.0	3175.0	3413.0	3500.0
	Inet.	(1040.0)	(1350.0)	(616.0)	(477.0)	(502.0)	(822.0)	(16000.0)
7th	Freq.	4800.0	5000.0	4950.0	4600.0	4538.0	4788.0	4825.0
	Inet.	(1220.0)	(1320.0)	(362.0)	(417.0)	(478.0)	(727.0)	(10700.0)

system is possible because the dynamic characteristics of the system change considerably depending on the position of partial coverage.

In Figure 14: (a) is the 2nd mode shape of the base beam. (b) shows a beam with partially-covered layers at the position of maximum displacement of the 2nd mode shape for vibration and damping control. Similarly, (c) and (d) are for vibration and damping control of the 3rd mode. The total weight of the constraining layer is one-third that of a completely covered beam.

Figure 15 shows the comparison of interances of completely-and partially-covered specimens cs1 and ps4. At the second resonant frequency, it is shown that the vibration and damping control by the partial coverage is more effective.

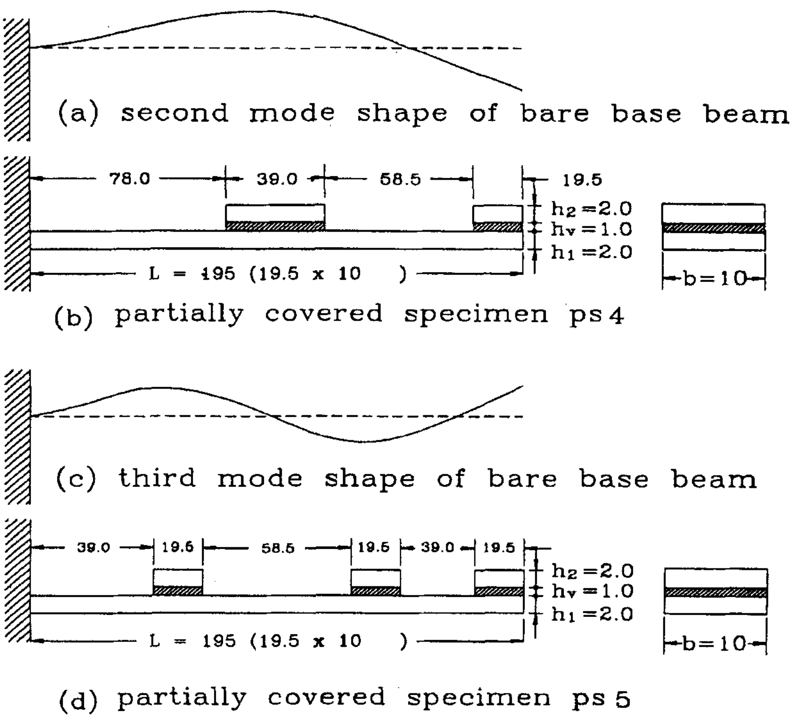

FIGURE 14 Mode shapes and geometry of partially-covered specimens.

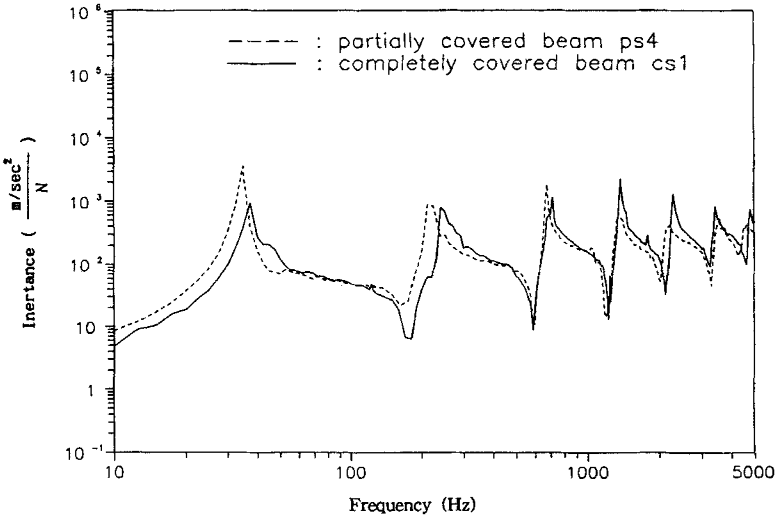

FIGURE 15 Comparison of transverse driving point inertances of completely- and partially-covered specimens cs1 and ps4.

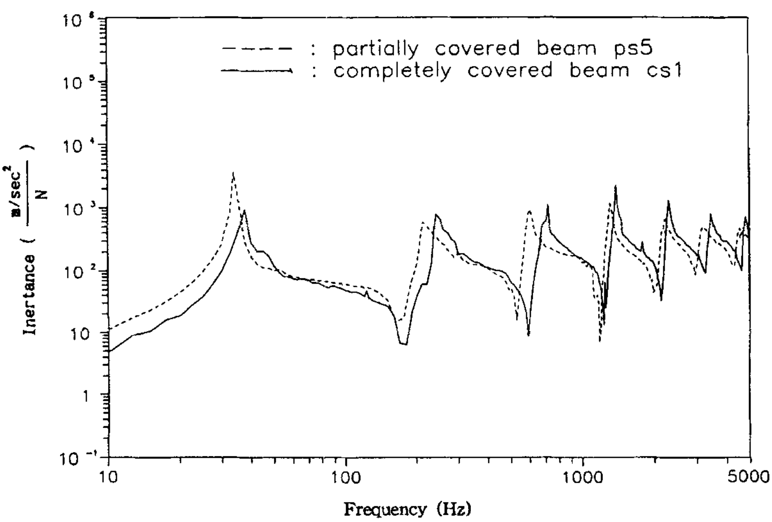

FIGURE 16 Comparison of transverse driving point inertances of completely- and partially-covered specimens cs1 and ps5.

Figure 16 indicates the effect of the partially-covered specimen ps5. If we compare Figure 16 with Figure 15, it shows the clear effect on the 3rd resonant frequency.

From the above mentioned results, it can be concluded that the damping capacity and the movement of the resonant frequencies of a partially-covered beam, with one or some constrained viscoelastic layers, are superior to those of a completely-covered beam. The efficiency depends on the position of the partial coverage. Therefore, if he vibrational characteristics of a system are known and it is necessary to control a specific mode, partial coverage can be a more effective approach than complete coverage.

5. CONCLUSIONS

The results of theoretical analysis and experiments on the sandwich beam with a viscoelastic core are as follows:

1) The fourth-order differential equations of motion are derived for the transverse vibration of completely- and partially-covered beams. The equations include both the transverse normal strain and the longitudinal shear strain of the viscoelastic layer. The transverse displacements of the constraining layer and the base beam are assumed to have different parameters. The steady state solution was solved as a boundary value problem applying the boundary and the continuity conditions. The results of the numerical calculations and experiments show good agreement.
2) If the partial coverage is positioned near the free edge of the cantilever beam. It can be more effective and economical for vibration and damping control than a completely-covered beam.
3) If the vibrational characteristics of a system are known and the partial coverage is located at the maximum displacement region of a mode shape, the vibration and damping effect can be maximized and the weight increment of a constraining layer can be minimized.

References

[1] DiTaranto, R. A., *Trans. ASME J. Appl. Mechanics* **32**, 881 (1965).
[2] Mead, D. J. and Markus, S., *J. Sound and Vibration* **10**, 163 (1969).

[3] Yan, M. J. and Dowell, E. H., *Trans. ASME J. Appl. Mechanics* **94**, 104 (1972).
[4] Douglas, B. E. and Yang, J. C. S., *AIAA J.* **16**, 925 (1978).
[5] Okazaki, A., Urata, Y. and Ookouchi, T., *JSME* **54**, 402 (1988).
[6] Okazaki, A., Urata, Y. and Ookouchi, T., *JSME* **54**, 2957 (1988).
[7] Rao, M. D. and Crocker, M. J., *Trans. ASME J. Vibration and Acoustics* **112**, 444 (1990).
[8] Plunkett, R. and Lee, C. T., *J. Acoust. Soc. America* **48**, 150 (1970).
[9] Okazaki, A. and Urata, Y., *JSME* **53**, 300 (1987).
[10] Dewa, H., Okada, Y. and Nagai, B., *JSME* **55**, 1575 (1989).
[11] Yuceoglu, U. and Updike, D. P., *ASCE J. Engr. Mech. Div.* **107**, 55 (1981).
[12] Ruzicka, J. E., *Structural Damping* (ASME, New York, 1959), pp. 49–87.
[13] Ramesh, T. C. and Ganesan, N., *J. Vibration and Acoust.* **117**, 213 (1995).
[14] Ewins, D. J., *Modal Testing: Theory and Practice* (John Wiley & Sons, New York, 1984), pp. 102–140.